Developing an Index to Measure Urban Heat Island Effect Using Satellite Land Skin Temperature and Land Cover Observations

MENGLIN S. JIN

Department of Meteorology and Climate Science, San Jose State University, San Jose, California

(Manuscript received 31 August 2011, in final form 8 March 2012)

ABSTRACT

A new index of calculating the intensity of urban heat island effects (UHI) for a city using satellite skin temperature and land cover observations is recommended. UHI, the temperature difference between urban and rural regions, is traditionally identified from the 2-m surface air temperatures (i.e., the *screen-level* temperature T_{2m}) measured at a pair of weather stations sited in urban and rural locations. However, such screen-level UHI is affected by the location, distance, and geographic conditions of the pair of weather stations. For example, choosing a different pair of rural and city sites leads to a different UHI intensity for the same city, due to the high heterogeneity of the urban surface temperature. To avoid such uncertainty, satellite-observed surface skin temperature measurements (i.e., *skin level* temperature T_{skin}) is recommended to record UHI, known as skin-level UHI or UHI_{skin}. This new index has advantages of high spatial resolution and aerial coverage to better record UHI intensity than T_{2m}. An assessment of skin-level UHI from 10 yr of the National Aeronautics and Space Administration (NASA)'s Moderate Resolution Imaging Spectroradiometer (MODIS) observations reveals that skin-level UHI has a strong UHI signal during the day and at night. In addition, there are significant diurnal and seasonal variations in skin-level UHI. Furthermore, the skin-level UHI is stronger during the day and summer (July) than during nighttime and winter. This new index is important for more uniformly assessing UHIs over cities around the globe. Nevertheless, whether the seasonality and diurnal variations revealed in this work using skin-level UHI index are valid over desert cities, such as Phoenix, Arizona, need to be examined.

1. Introduction

Urban heat island effects (UHI) are defined by temperatures in urban regions exceeding those in surrounding rural regions. Traditionally, the UHI is quantified as the difference between the 2-m surface air temperature T_{2m} of a screen-level weather station (e.g., a World Meteorological Organization site) located in an urban region and T_{2m} for a nearby rural weather station. First reported by Howard (1833), the UHI has been studied for decades (Landsberg 1970; Oke 1982; Arnfield 2003; Yow 2007; Jin and Shepherd 2005, 2008; Zhou and Shepherd 2009). There are two key features associated with this screen-level UHI: 1) urban T_{2m} is higher than rural T_{2m} and 2) the UHI is maximum at night or during early morning, and thus the UHI has been called a "nocturnal phenomenon" (Oke 1982). The general explanation of this nighttime phenomenon is that buildings and roads store heat during the daytime and at nighttime, these surfaces emit heat back to the atmosphere, increasing the 2-m air temperature (Grimmond and Oke 1999).

New observations from satellite remote sensing should be helpful to advance our understanding of the UHI because of the following:

1) Traditional UHI studies use T_{2m} observations from one or a few sites over urban and surrounding rural regions (referred to as UHI_{2m} or screen-level UHI in this paper). The microthermal properties of a city vary with the complex surface structure, creating extreme heterogeneity in T_{2m}. Therefore, using one site to represent the city temperature is generally problematic.
2) The surrounding areas of a city can have different land cover types. For example, there are four different types of land cover (mixed forest, open shrubland, croplands, savanna) around Beijing (BJ), China. Even though WMO sites are required to be sited over short grass (Maidment 1993), the different surrounding land

Corresponding author address: Dr. Menglin S. Jin, Dept. of Meteorology and Climate Science, San Jose State University, 1 Washington Square, San Jose, CA 95120.
E-mail: jin@met.sjsu.edu

DOI: 10.1175/JCLI-D-11-00509.1

covers lead to different T_{2m} measurements. Therefore, a rural station may not accurately represent the surrounding rural temperature for different types of land cover.

Simply put, the magnitude of UHI_{2m} depends on the locations of the city and rural observations, complicating the assessment of the spatiotemporal attributes of UHI and making it impossible to compare the UHI of one city to another.

The UHI has also been detected using relatively high-resolution satellite observations of the land surface skin temperature T_{skin} (Voogt and Oke 1997; Jin et al. 2005, 2011), which is generally reported as higher in urban areas than in surrounding regions. However, a desert city, such as Phoenix, Arizona, may be observed as colder than the rural surroundings (Jin et al. 2005). This *skin-level* UHI (or UHI_{skin}) is an important concept because T_{skin} has a different magnitude and physical meaning than T_{2m} (Jin et al. 1997; Jin 2004; Jin and Dickinson 2010). Therefore, high-resolution and high spatial coverage satellite data lead to a more objective method to assess UHI, and thus they can be comparable to all global cities.

2. Data

The National Aeronautics and Space Administration (NASA)'s Moderate Resolution Imaging Spectroradiometer (MODIS; King et al. 2003) remotely sensed data are used as a prototype to study UHI_{skin}. The MODIS instrument is currently deployed on NASA's *Terra* and *Aqua* satellites; however, the UHI_{skin} can be calculated from other satellite observations as well.

Skin temperature (T_{skin}) is measured in seven solar and three thermal spectral bands of MODIS at 1030 LT and 2230 LT (*Terra*), and 1330 LT and 0130 LT (*Aqua*) daily. Each pixel has ~1-km resolution at nadir (Wan and Dozier 1996; Wan and Li 2008). The measurements used in this study have been rescaled to a 5-km resolution (or so-called 0.05° latitude–longitude MODIS resolution) and averaged to monthly values. Only measured values with quality flags attesting to the absence of clouds are used. Corresponding land cover data (Friedl et al. 2002) are used to identify urban and rural pixels. All MODIS data used here are collection version 5.

3. Methodology

Radiometric T_{skin} retrieved by satellite-based instruments is derived from the longwave radiation emitted from the underlying surface within an instantaneous field of view (FOV), after corrections for atmospheric and surface emissivity effects (Prata et al. 1995; Jin and Dickinson 1999, 2000). The advantages of satellite T_{skin} measurements include high spatial resolution, large aerial coverage, and high quality. First, we define

$$UHI_{skin} = T^{u}_{skin} - T^{r}_{skin,LC}, \quad (1)$$

where UHI_{skin} is the skin-level UHI, T^{u}_{skin} is the skin temperature averaged from all urban pixels for a given region, and $T^{r}_{skin,LC}$ is the skin temperature averaged from all rural pixels in the region for a specific land cover (LC). Since rural areas often have different land cover, UHI depends on which rural land cover is selected for comparison with urban areas. Normally, to be consistent with UHI_{2m}, cropland is selected when available as the land cover for comparing with the urban area. However, for some cities, there is no cropland nearby and thus one needs to make it clear which land cover is used in the UHI_{skin} calculation.

Note that as defined in Eq. (1), UHI_{skin} is an area-averaged index. This study chooses a 0.6° × 0.6° grid box, partly because this size includes an adequate number of pixels and partly because other size boxes show a similar UHI signal. This area-averaged index reduces the uncertainty caused by urban surface heterogeneity, since UHI_{skin} can examine all urban T_{skin} within an area. Note that other box sizes are also analyzed, specifically boxes of size 0.5° × 0.5°, 0.8° × 0.8°, 1.0° × 1.0°, and 2.0° × 2.0°. The features are very similar and thus only results from the 0.6° × 0.6° box are presented in this paper.

Deployed on polar-orbiting satellite platforms, *Terra* observes a given area twice per day (1030 and 2230 LT) and *Aqua* also observes the same area twice per day (1330 and 0130 LT). Therefore, for a specific area, four T_{skin} observations are available daily under clear-sky conditions. With such a dataset, the diurnal, seasonal, and interannual variations of skin-level UHI are examined in this study.

4. Results

a. UHI_{skin} versus land cover

Sixteen land cover types are remotely sensed by MODIS to reveal surface physical features, even for highly heterogeneous land surfaces (see Table 1). The land covers of Beijing, New York City (NYC), New York, and their surrounding areas are determined from the 0.05° latitude–longitude MODIS-observed land cover dataset (Figs. 1a and 1b). The urban land covers for Beijing and NYC are the red mapped areas (LC = 13, urban); however, note that the surrounding environments of these two large cities are not similar. NYC is a coastal location (LC = 0) with the surrounding inland regions

TABLE 1. MODIS land cover (LC).

	LC type
1	Evergreen needleleaf forest
2	Evergreen broadleaf forest
3	Deciduous needleleaf forest
4	Deciduous broadleaf forest
5	Mixed forest
6	Closed shrubland
7	Open shrubland
8	Woody savannas
9	Savannas
10	Grassland
11	Permanent wetland
12	Croplands
13	Urban and built-up
14	Cropland/natural vegetation mosaic
15	Snow and ice
16	Barren or sparsely vegetated

covered by deciduous broadleaf forest (LC = 4). By comparison, the area north of Beijing is a mountainous region with land cover including mixed forest (LC = 5); other surrounding regions include cropland (LC = 12), open shrubland (LC = 7) and savannas (LC = 9). These differences suggest that, although both Beijing and NYC are large cities at similar latitudes, the UHI may be different for the two cities due to differences in surrounding land cover and distance from the coast.

In July 2008, the central high-building regions of Beijing have a monthly-mean T_{skin} above 308 K (Fig. 1c). This is significantly higher than the surrounding nonurban regions, where the cropland-dominated landscape has T_{skin} values in the 302–304-K range. The forests north of Beijing have T_{skin} as low as 298–300 K. This 4–8-K monthly average difference between a city and a rural region suggests a significant energy need for air conditioning in the city. By comparison, NYC (Fig. 1d) also has a maximum monthly-mean T_{skin} above 308 K, while the nonurban area T_{skin} is as low as 300–302 K. The *Terra* daytime observations (1030 LT) used here confirm that the daytime UHI_{skin} is significant for both Beijing and NYC.

The area-averaged T_{skin} indicates a significant UHI for both Beijing and NYC (Fig. 2). For July 2008, within a 0.6° × 0.6° box over Beijing (39.7°–40.3°N, 116.1°–116.7°E), urban-pixel-averaged T_{skin} is higher than other land-cover-averaged T_{skin}. In this box, 57.4% of the pixels are urban cover (LC = 13), about 30.1% are cropland (LC = 12), 8.2% are savanna (LC = 9), and 6.7% are mixed forest. Open shrubland (LC = 7) also exists but with a very small percentage. The mean value of T_{skin} is about 306 K for urban-pixel-averaged Beijing, 304.4 K for cropland, 303.2 K for savanna, 300.6 K for open shrubland, and 300.0 K for mixed forest.

The area surrounding NYC is different than that around Beijing. Generally, water and mixed forest areas are next to the 0.6° × 0.6° box for NYC urban areas (40.5°–41.1°N, 73.8°–74.4°W, Fig. 2c). In July 2008, the monthly-mean T_{skin} is 304.5 K for NYC and 299.2 K for the mixed forest; thus, the UHI_{skin} is about 5.5 K. The same analyses are also conducted at other box sizes; that is, 0.5° × 0.5°, 0.8° × 0.8°, 1.0° × 1.0°, and 2.0° × 2.0°, and similar UHI_{skin} features are observed (not shown).

b. Diurnal variation of UHI

The diurnal variation of skin-level UHI is significant for Beijing (Fig. 3), with a larger UHI signal observed during the daytime than during the nighttime. At night, both 2230 LT (*Terra* nighttime) and 0130 LT (*Aqua* nighttime) observations of T_{skin} are similar, with a peak T_{skin} value of about 297 K over central urban regions (around 116.3°–116.4°E) and about 294.5 K over cropland (116.6°–117.4°E). Therefore, the UHI_{skin} effect is roughly a 2.5-K difference between urban land cover and cropland at night. During the day, both 1330 LT (*Aqua* daytime) and 1030 LT (*Terra* daytime) urban T_{skin} is higher than that of the surrounding cropland (difference exceeding 4.5 K). Note that even for the same land cover type, T_{skin} can vary by several degrees. For example, for *Terra* daytime (1030 LT), the difference over cropland ranges from 305.0 K at 116.6°E to 300.0 K at 117.4°E. Therefore, a difference of 5 K can be induced for UHI_{skin} simply because of the T_{skin} difference over the same cropland cover. At 116.0°E, land cover is mixed forest and T_{skin} is 302.5 K at 1330 LT, while the T_{skin} of the urban regions is 310.8 K. Similarly, at 1030 LT, T_{skin} for the urban land cover is 307.5 K, while T_{skin} over mixed forest at 116.0°E is 300.6 K, which is a UHI_{skin} effect of 7 K for forest land cover. More importantly, this cross-section display of T_{skin} over urban and nearby land cover suggests that an area-averaged signal of UHI might be most proper because T_{skin} can be different for the same city and for the same surrounding land cover.

c. Seasonality of UHI

In all seasons, along the latitude of 40°N and from 116° to 118°E longitude, urban T_{skin} for Beijing is higher than that of all other land covers (Fig. 4a). Specifically, in July 2007 monthly-mean T_{skin} peaks at 308.5 K over the central urban region (~116.3°E), while for the mixed forest regions (116.0°E) it is 300.0 K, and for nearby savannas (~116.8°E) it is 301.5 K. The cropland monthly-mean T_{skin} is in the range of 300.0–302.0 K, which is lower than urban regions but higher than mixed forest (116.0°E).

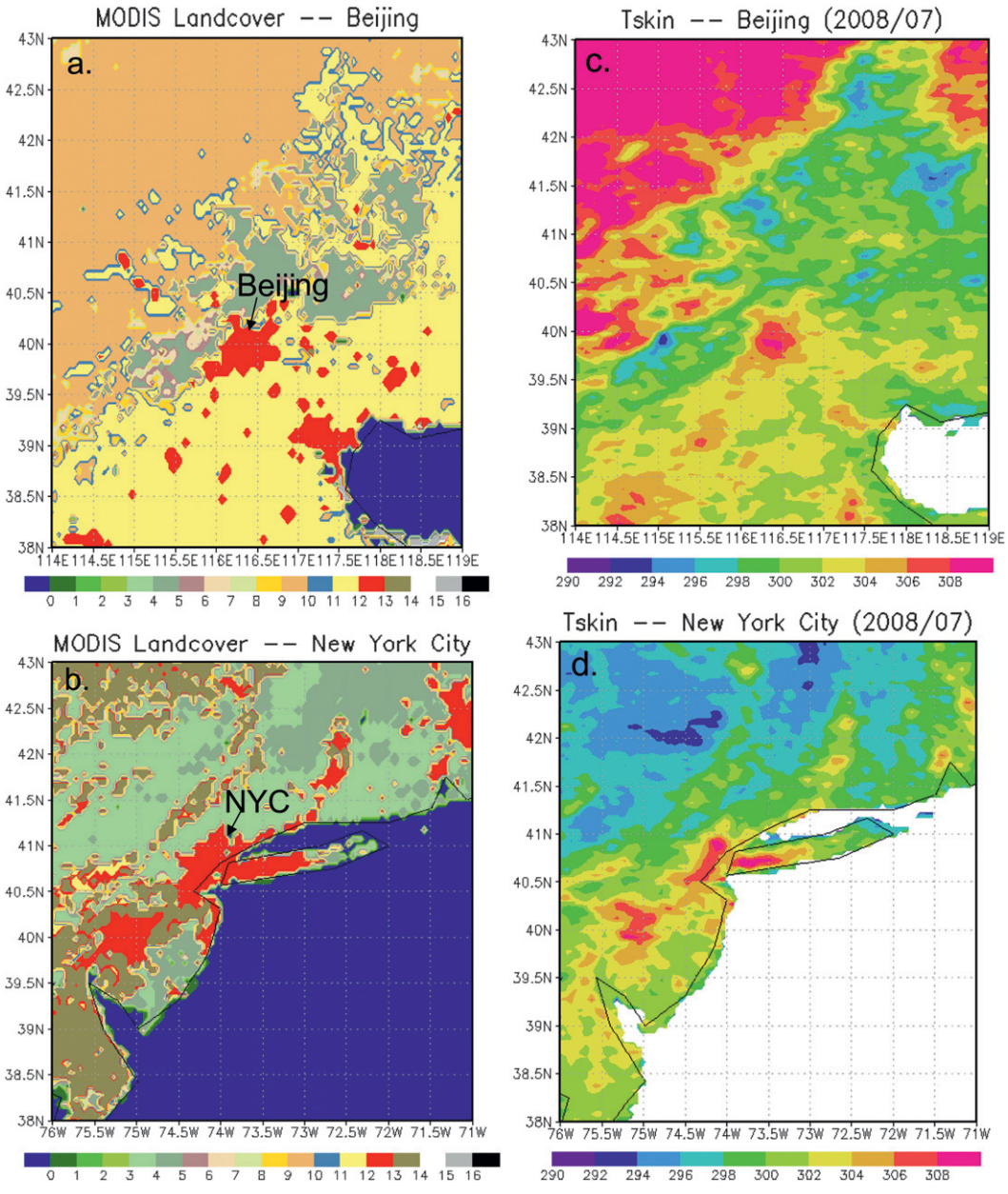

FIG. 1. LC of (a) BJ and (b) NYC based on MODIS observation of July 2007. LC type is given in Table 1. LC = 13 is urban (red). BJ and NYC are marked. Spatial observations of T_{skin} for (c) BJ and (d) NYC for July 2008. The unit is K, and the data are monthly observations from MODIS *Terra* at 1030 LT.

In April, the monthly-mean T_{skin} is much lower than in August but higher than in October or January. The differences between April and October are about 2 K for mixed forest (116.0°E) and 5–7 K for cropland or urban regions. In January, all land covers experience lower monthly-mean T_{skin}, mainly due to the low surface insolation in winter. More importantly, the winter UHI_{skin} is not as evident as it is in other seasons. For example, the monthly averaged T_{skin} for the urban pixels at 116.3°–116.5°E is 276.4 K, while for the savannas (116.8°–116.9°E) it is 276 K. The T_{skin} for the cropland at 117.3° and 117.7°E is above 275 K. More specifically, from 116.3° to 117.0°E, there is little difference in T_{skin}, although the land cover types are urban (LC = 13), cropland (LC = 12), and savanna (LC = 9). Therefore, the winter UHI is not as evident as in other seasons, at least for this specific city. In fact, the sign is sometimes opposite (so-called urban cooling), meaning that the rural region can be warmer than

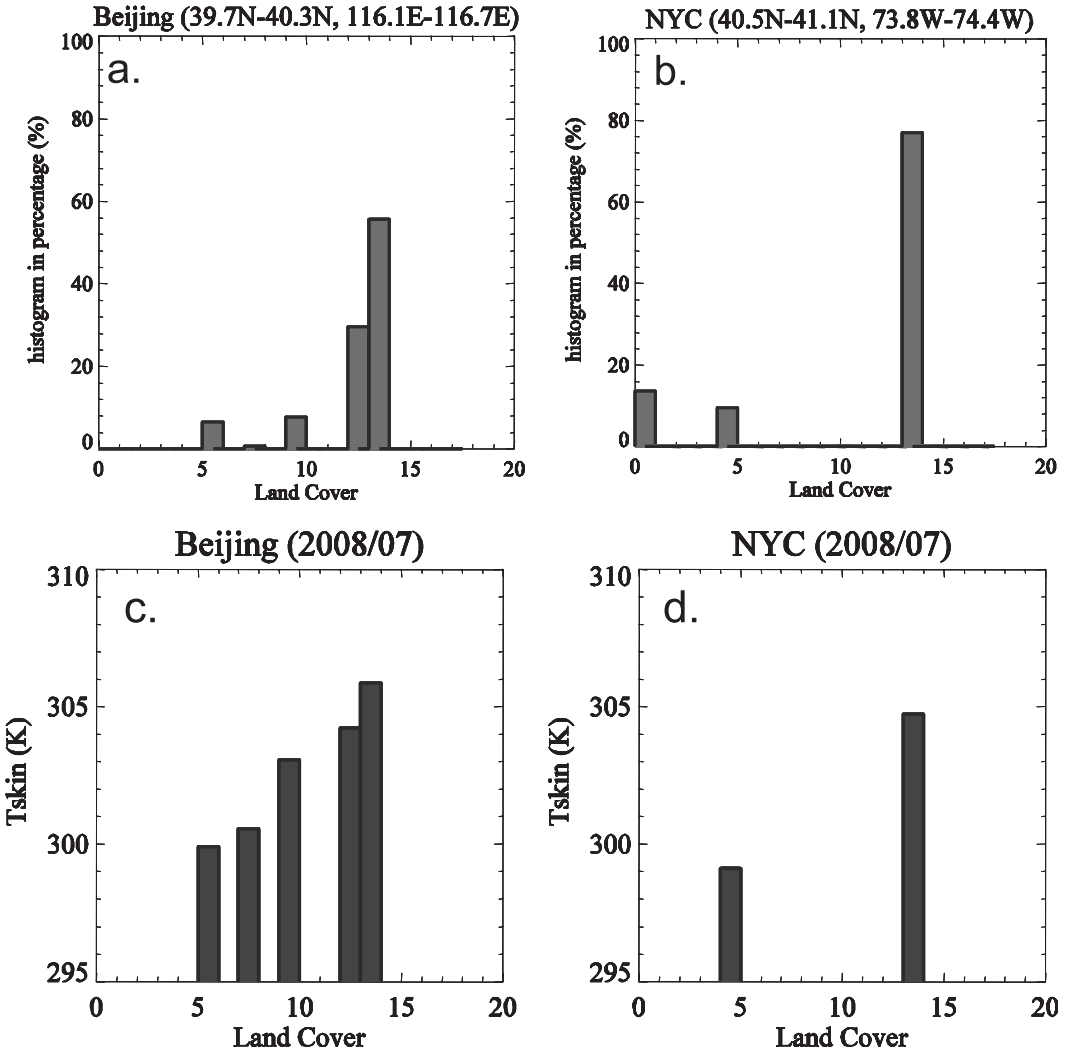

FIG. 2. LC and skin temperature averaged for a 0.6° × 0.6° box over BJ and NYC. LC percentage for (a) BJ and (b) NYC. LC = 13 is urban (see Table 1). The 0.6° × 0.6° box is 39.7°–40.3°N, 116.1°–116.7°E for BJ and 40.5°–41.1°N, 73.8°–74.4°W for NYC. The 0.6° × 0.6° box-averaged land surface skin temperature for (c) BJ and (d) New York City. In (d), LC = 0 means ocean, and thus there is no skin temperature value for ocean from MODIS land surface products; T_{skin} is observed from *Terra* data at 1030 LT.

certain parts of the city. This ''urban cool island'' phenomenon warrants further study.

Similar to Beijing, New York City has a clear seasonal UHI signal (Fig. 4b). *Terra* daytime (1030 LT) observations show that in July, T_{skin} peaks at 302.0–304.0 K for urban regions and 296.0–298.0 K for deciduous broadleaf forest (LC = 4, around 74.5°W). This 6-K difference is comparable with that of Beijing. Furthermore, the UHI is evident in other seasons, although the magnitude is less than that of July. Specifically, the UHI between urban and deciduous broadleaf forests (LC = 4) is 3 K for April (295 K urban vs 292 K forest), 2 K for October (288 K urban vs 286 K forest), and 2 K for January (274 K urban vs 272 K forest). In this case, UHI is significant even in winter.

d. Interannual variations of UHI

Interannual variation of UHI is evident. For example, in July 2007, Beijing (Fig. 4a) is warmer than in July 2008, while surface cropland areas (116°–118°E) are colder than in 2008. This leads to a larger UHI_{skin} in July 2007 than in July 2008. Nevertheless, although July 2007 has a relatively higher temperature, the overall pattern does not change. This suggests that the UHI is evident even though it has interannual variations.

e. Statistical analysis

Because the observations have a 10-yr duration, a statistical approach is helpful to reveal the significance of

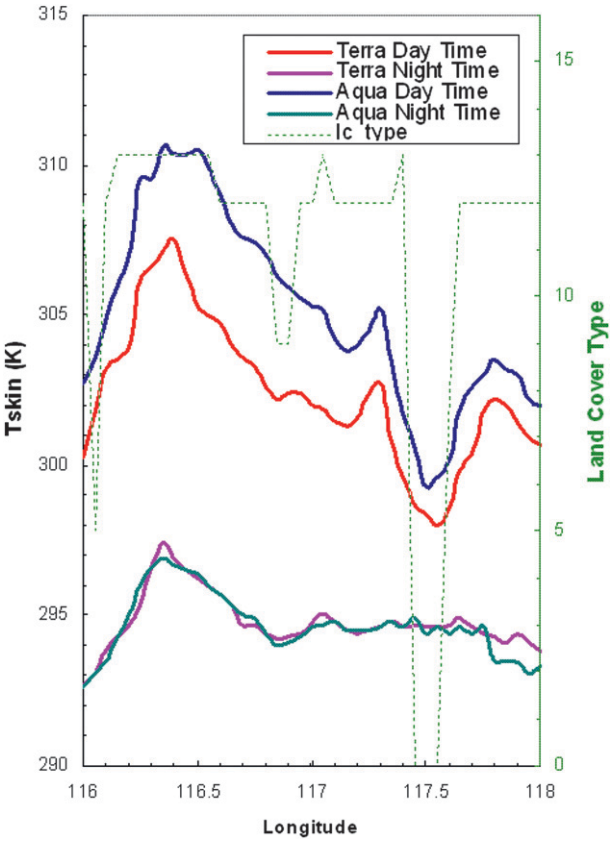

FIG. 3. Monthly-mean skin temperature in July 2008 for BJ observed by *Terra* daytime (1030 LT), *Aqua* daytime (1330 LT), *Terra* nighttime (2230 LT), and *Aqua* nighttime (0130 LT). LC type (defined in Table 1) is presented along the longitude 116°–118°E as a dashed line.

UHI for all months from April 2000 to December 2008 (for a total of 105 samples). The box plot (Fig. 5a; Wilks 1995), or box-and-whisker plot, identifies the five important statistics on this time series (April 2000–December 2010): the 75th percentile, the 25th percentile, the 50th percentile (or median), and the maximum and minimum values. Beijing T_{skin} is higher than that of surrounding land covers for all five statistics. The median T_{skin} of the Beijing region is 297.5 K, higher than any of the other four land covers (mixed forest, open shrubland, savannas, and cropland). More importantly, Beijing has the highest T_{skin}, above 312.0 K. In addition, the 75th percentile of T_{skin} is 304.6 K, higher than for the other land covers. This implies that the urban area is a possible place for extreme heat waves to occur due to UHI mechanisms.

A similar box plot (Fig. 5b) is produced for New York City (Fig. 5b), and the same conclusion is observed, namely, the mean difference between NYC and the surrounding forest being 3.75 K. NYC is hotter than the forest for all five statistics. As a result, the UHI is evident for NYC.

A *t* test (not shown) is also used to examine the statistical significance of the UHI signal and it proves that, statistically, Beijing and NYC are hotter than the surrounding regions over the entire year with 95% confidence.

5. Discussion

The UHI is evident from the radiative surface skin temperature field. There is clear diurnal variation in UHI_{skin}, with a larger UHI intensity during daytime than during nighttime. There is also a seasonal variation in UHI_{skin}, with a larger signal in summer than in winter. This seasonal variation corresponds to the seasonality of solar radiation, the vegetation growing cycle, and rainfall or soil moisture content.

UHI_{skin} maximizes during the daytime. Therefore, we should not consider UHI exclusively a "nighttime phenomenon" anymore. Jin et al. (2005) suggested the possible physical mechanisms responsible for a stronger daytime UHI: the albedo is reduced in urban regions, partly due to urban canopy effect and partly due to new materials used in urban roads and buildings; consequently, more solar radiation is absorbed at the surface to warm it. In addition, surface emissivity is reduced because of the new materials used in the urban surface, leading to less longwave radiation leaving the surface. As a result, daytime UHI is stronger than nighttime UHI. Furthermore, urban regions reduce soil moisture and vegetation coverage, which further change the solar radiation redistribution in terms of latent and sensible heat fluxes (e.g., Bowen ratio), and thus increases surface temperature. MODIS provides albedo data (Schaaf et al. 2002), emissivity data (Jin and Liang 2006), and vegetation data (Myneni et al. 1995), which can be further used to address these mechanisms.

Why is it that from T_{2m} data, the maximum UHI occurs at night as other scientists have reported (Oke 1982), but from satellite T_{skin} data, UHI occurs at both day and night? Previous and current work using T_{skin} shows an even larger UHI signal during daytime than nighttime (Jin et al. 2005). Several hypotheses are proposed here for such a difference: First, T_{skin} and T_{2m} are two different physical variables representing the heat transport from the ground to the near surface (Jin and Dickinson 2002, 2010). Also, T_{skin} has a fast response to surface insolation, while T_{2m} is not as sensitive to disturbance in surface insolation (Jin and Dickinson 2010). During the daytime, T_{skin} increases very quickly and then heats up the 2-m air layer. Second, at nighttime, the boundary layer is stable and heat is trapped in the warm near-surface air layer.

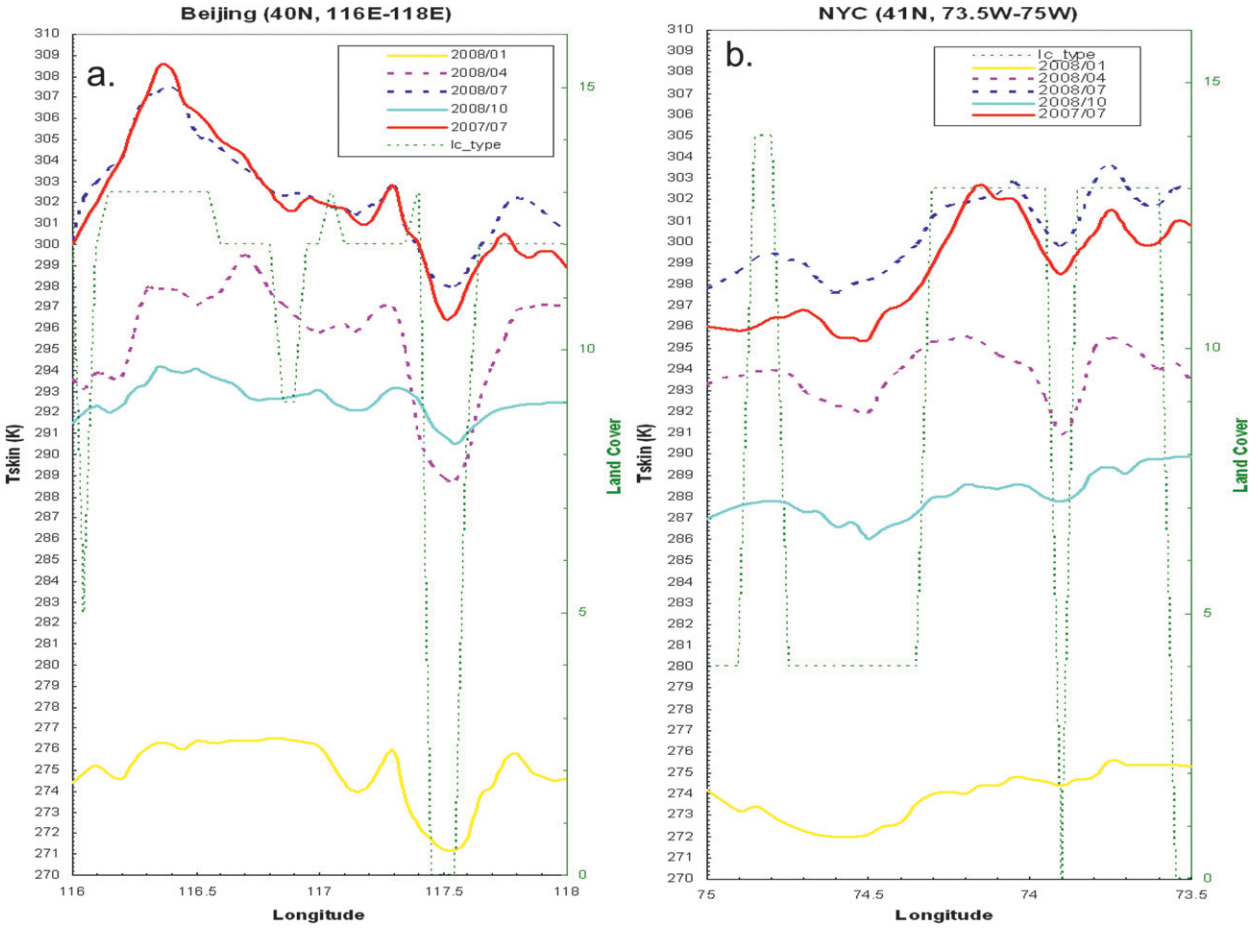

FIG. 4. (a) Monthly-mean skin temperature from January, April, July, and October 2008 together with July 2007 for BJ. LC type (defined in Table 1) is also presented along the longitude 116°–118°E. Data are from *Terra* MODIS. (b) Monthly-mean skin temperature from January, April, July, and October 2008 together for NYC. Land cover type (LC, defined in Table 1) is also presented along the longitude 75°–73.5°W. Data are from *Terra* MODIS.

Therefore, the UHI signal can be detected at T_{2m}. During the daytime, convection is strong and thus the UHI is not very evident at the 2-m air layer. Third, uncertainty exists in the traditional T_{2m} index. For example, UHI T_{2m} heavily depends on the locations of the rural and urban weather stations, and thus it may miss the maximum UHI signal. Further research is needed to examine these hypotheses. Furthermore, Shen and Leptoukh (2011) show that the largest differences between T_{2m} and T_{skin} occur at daytime over barren areas. Therefore, simply using T_{2m} may miss the important signal of the UHI.

The UHI_{skin} provides additional information to complement the traditional T_{2m} screen-level UHI. Nevertheless, we cannot ignore screen-level UHI nor try to replace the latter with the former because of the following reasons:

1) Skin-level and screen-level UHI have different UHI intensities, which reflect the skin-surface and near-surface atmosphere interactions. Both UHI definitions are important in calculating the surface energy budget.
2) Screen-level UHI has a long climatological record, which is essential for the study of the change in UHI related to city growth.
3) Skin temperature has the advantage of broader coverage; but, it is only available for clear days (Jin and Dickinson 2010). Therefore, skin-level UHI may not fully represent heat intensity during all sky conditions. It would be instructive to assess the skin-level UHI for all sky conditions (clear and cloud sky) but that is currently not possible, via thermal infrared remote sensing, due to the lack of satellite T_{skin} observations for cloudy skies.

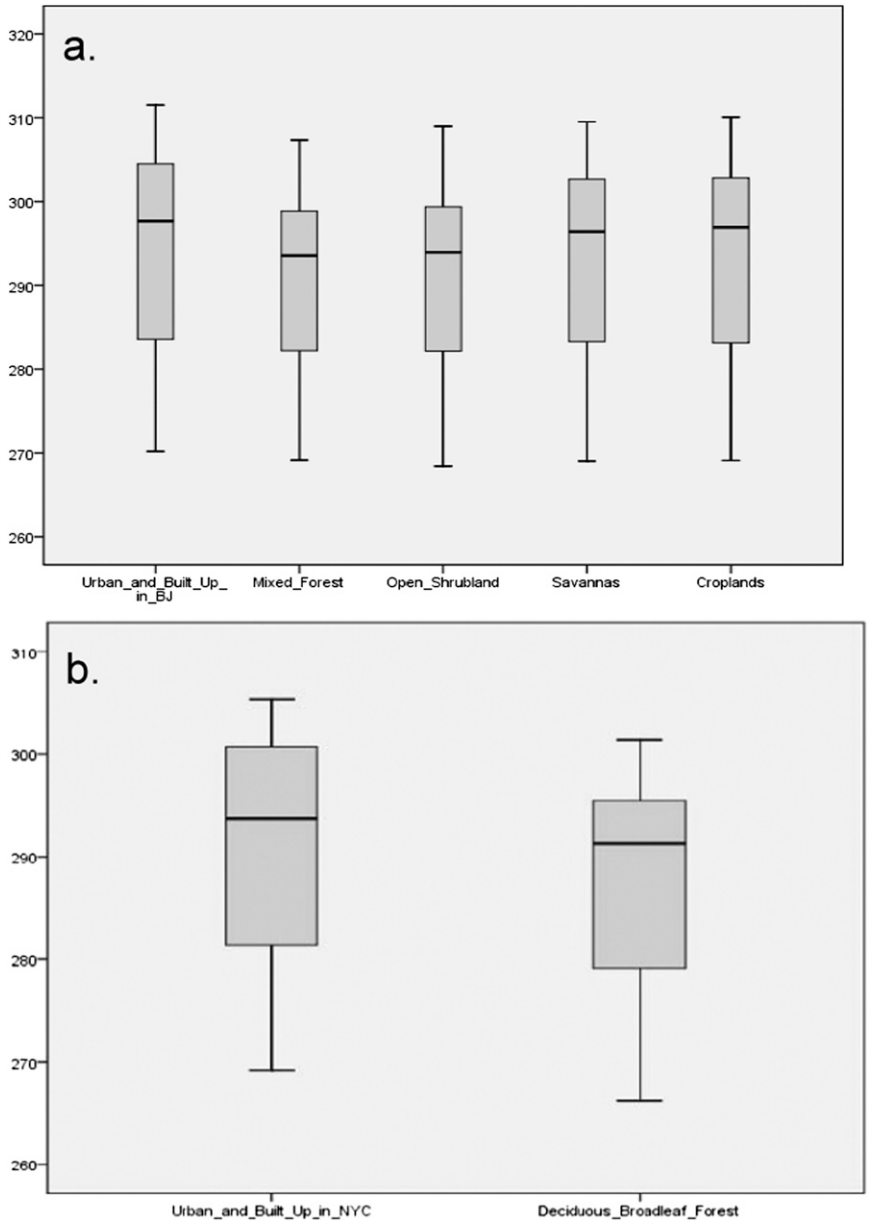

FIG. 5. Box plot based on April 2000–December 2008 skin temperature observations over the 0.6° × 0.6° selected box of (a) BJ and surrounding land cover regions and (b) NYC. A total of 105 monthly values are examined. The top of the box represents the 75th percentile, the bottom of the box represents the 25th percentile, and the line in the middle represents the 50th percentile (i.e., median). The whiskers (the lines that extend out the top and bottom of the box) represent the highest and lowest values that are not outliers or extreme values (Wilks 1995).

In conclusion, both screen-level and skin-level UHIs are important for a complete understanding of urban heat distribution, local and regional circulation, and water and heat cycles.

Acknowledgments. This work is funded by NSF GEO/ATM/LARS/Climate and Large-Scale Dynamics Program Award 0855480 and NASA Precipitation Program Grant NNX10AH65G.

REFERENCES

Arnfield, A. J., 2003: Two decades of urban climate research: A review of turbulence, exchanges of energy and water, and the urban heat island. *Int. J. Climatol.,* **23,** 1–26.

Friedl, M. A., and Coauthors, 2002: Global land cover mapping from MODIS: Algorithms and early results. *Remote Sens. Environ.,* **83,** 287–302.

Grimmond, C. S. B., and T. R. Oke, 1999: Heat storage in urban areas: Local-scale observations and evaluation of a simple model. *J. Appl. Meteor.,* **38,** 922–940.

Howard, L., 1833: *The Climate of London: Deduced from Meteorological Observations, Made in the Metropolis, and at Various Places around It*. 2nd ed. Vol. 1, Harvey and Darton, 348 pp.

Jin, M., 2004: Analyzing skin temperature variations from long-term AVHRR. *Bull. Amer. Meteor. Soc.,* **85,** 587–600.

——, and R. E. Dickinson, 1999: Interpolation of surface radiative temperature measured from polar orbiting satellites to a diurnal cycle. Part 1: Without clouds. *J. Geophys. Res.,* **104** (D2), 2105–2116.

——, and ——, 2000: A generalized algorithm for retrieving cloudy sky skin temperature from satellite thermal infrared radiances. *J. Geophys. Res.,* **105** (D22), 27 037–27 047.

——, and ——, 2002: New observational evidence for global warming from satellite. *Geophys. Res. Lett.,* **29,** 1400, doi:10.1029/2001GL013833.

——, and J. M. Shepherd, 2005: Inclusion of urban landscape in a climate model: How can satellite data help? *Bull. Amer. Meteor. Soc.,* **86,** 681–689.

——, and S. Liang, 2006: An improved land surface emissivity parameter for land surface models using global remote sensing observations. *J. Climate,* **19,** 2867–2881.

——, and J. M. Shepherd, 2008: Aerosol relationships to warm season clouds and rainfall at monthly scales over east China: Urban land versus ocean. *J. Geophys. Res.,* **113,** D24S90, doi:10.1029/2008JD010276.

——, and R. E. Dickinson, 2010: Land surface skin temperature climatology: Benefitting from the strengths of satellite observations. *Environ. Res. Lett.,* **5,** 044004, doi:10.1088/1748-9326/5/4/044004.

——, ——, and A. M. Vogelmann, 1997: A comparison of CCM2–BATS skin temperature and surface-air temperature with satellite and surface observations. *J. Climate,* **10,** 1505–1524.

——, ——, and D.-L. Zhang, 2005: The footprint of urban areas on global climate as characterized by MODIS. *J. Climate,* **18,** 1551–1565.

——, W. Kessomkiat, and G. Pereira, 2011: Satellite-observed urbanization characters in Shanghai, China: Aerosols, urban heat island effect, and land–atmosphere interactions. *Remote Sens.,* **3,** 83–99, doi:10.3390/rs3010083.

King, M. D., and Coauthors, 2003: Cloud and aerosol properties, precipitable water, and profiles of temperature and humidity from MODIS. *IEEE Trans. Geosci. Remote Sens.,* **41,** 442–458.

Landsberg, H. E., 1970: Man-made climate change. *Science,* **170,** 1265–1274.

Maidment, D. R., 1993: *Handbook of Hydrology*. McGraw-Hill, Inc., 1424 pp.

Myneni, R. B., F. G. Hall, P. J. Sellers, and A. L. Marshak, 1995: The interpretation of spectral vegetation indexes. *IEEE Trans. Geosci. Remote Sens.,* **33,** 481–486.

Oke, T. R., 1982: The energetic basis of the urban heat island. *Quart. J. Roy. Meteor. Soc.,* **108,** 1–24.

Prata, A. J., V. Caselles, C. Colland, J. A. Sobrino, and C. Ottlé, 1995: Thermal remote sensing of land surface temperature from satellites: Current status and future prospects. *Remote Sens. Rev.,* **12,** 175–224.

Schaaf, C. B., and Coauthors, 2002: First operational BRDF, albedo nadir reflectance products from MODIS. *Remote Sens. Environ.,* **83,** 135–148.

Shen, S. and G. G. Leptoukh, 2011: Estimation of surface air temperature over central and eastern Eurasia from MODIS land surface temperature. *Environ. Res. Lett.,* **6,** 045206, doi:10.1088/1748-9326/6/4/045206.

Voogt, J. A., and T. R. Oke, 1997: Complete urban surface temperatures. *J. Appl. Meteor.,* **36,** 1117–1132.

Wan, Z. M., and J. Dozier, 1996: A generalized split–window algorithm for retrieving land–surface temperature from space. *IEEE Trans. Geosci. Remote Sens.,* **34,** 892–905.

——, and Z.-L. Li, 2008: Radiance-based validation of the V5 MODIS land-surface temperature product. *IEEE Trans. Geosci. Remote Sens.,* **29,** 5373–5395.

Wilks, D. S., 1995: *Statistical Methods in the Atmospheric Sciences: An Introduction*. Academic Press, 467 pp.

Yow, D. M., 2007: Urban heat islands: Observations, impacts, and adaptation. *Geogr. Compass,* **1,** 1227–1251.

Zhou, Y., and J. M. Shepherd, 2009: Atlanta's urban heat island under extreme heat conditions and mitigation strategies. *Nat. Hazards,* **52,** 639–668, 10.1007/s11069-009-9406-z.